Calibrating the South Pole Telescope-Sunyaev-Zel'dovich Cryostat for Future Detector Wafer Testing

Agustin Garcia Flores[1,2*], Paul Chichura[3], Sasha Rahlin[3], Tyler Natoli[3], Thomas Crawford[3], Bradford A. Benson[3*]

[1]Department of Applied Phyiscs and Materials Science, Northern Arizona University, Flagstaff, AZ 85011, USA

[2]Department of Physics, Arizona State University, Tempe, AZ 85281, USA

[3]Department of Astronomy and Astrophysics, University of Chicago, Chicago, IL 60637, USA

To investigate the Cosmic Microwave Background, the detectors must be very properly calibrated and kept in a noise-free environment. In order to prepare for a graduate student instrumentation summer school, the cryostat that holds the detectors must be fully operational and efficient. The cryostat's stability can be determined by performing preliminary tests (in the form of cryostat cool-downs) and seeing how it behaves. Temperatures will be recorded throughout the test cool-downs to determine whether the cryostat is ready for the load of additional detectors. In the end, the temperatures recorded during the test cool-downs were even lower than anticipated. After integrating all of the equipment that would be used during the instrumentation summer school, a base temperature of 253 mK was determined for the cryostat. The test cool-downs demonstrated that the cryostat was still operating at full capacity despite the fact that it had not been used in several years.

1 Introduction

The beginning of time can reveal details about how the early cosmos came to be. It sheds light on the formation and structure of galaxies. For years, cosmologists have wanted to know this information, as any knowledge concerning it would be a huge success for the entire study of cosmology.

In 1965, while working with a newly constructed radio antenna, Arno Penzias and Robert Wilson of AT&T Bell Laboratories observed an extremely strong, uniform signal streaming in from all directions. This signal was once assumed to be nothing more than a mechanical problem with the radio antenna. At the same time, a team led by Princeton University's Robert Dicke actively searched for the Cosmic Microwave Background (CMB). Dicke and his crew learned about Penzias and Wilson's problems with an unknown uniform signal and realized that the CMB had been discovered (Sobrin et al. (2022)).

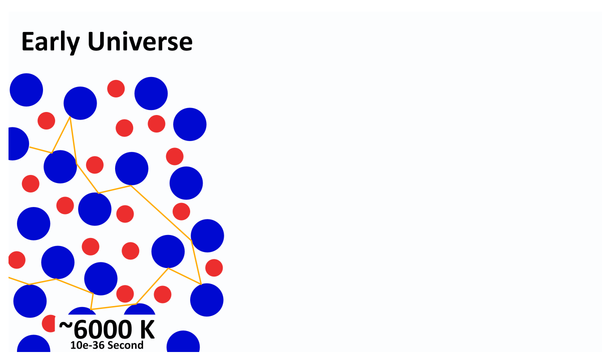

Figure 1: 10e−36 seconds after the Big Bang, any and all atoms were broken apart into protons, electrons, and neutrons due to the tremendous temperatures. As a result, photons at the time were constantly scattered, making it impossible to trace them back to their source.

The CMB began with time, it is made up of photons that were trapped in the very early stages of the cosmos. Because of the cosmos' expansion and cooling, these photons were eventually able to escape and freely explore the universe.

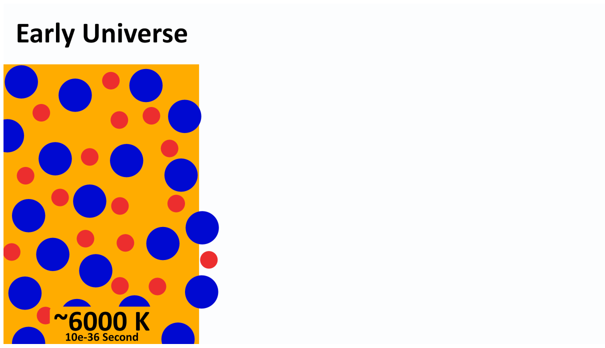

Figure 2: This is regarded as the universe's bright stage. All photons were effectively imprisoned in a cloud of protons, electrons, and neutrons.

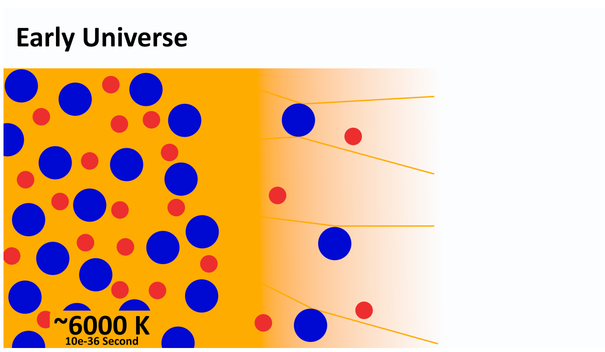

Figure 3: As time passed, the cosmos stretched and began to cool. The gap between protons, electrons, and neutrons was expanding, allowing photons to escape.

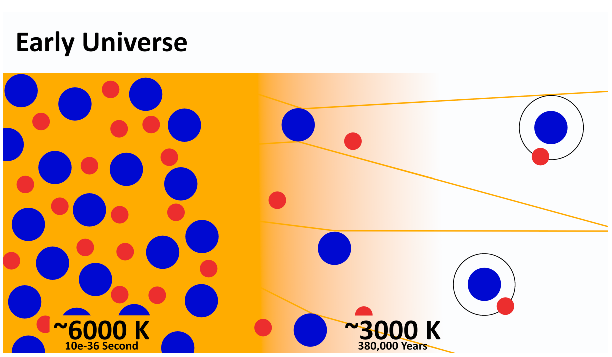

Figure 4: The universe eventually become "transparent." Hydrogen atoms were forming, and photons could flow freely through space.

During the early phases of the cosmos, the wavelength of the CMB was around 600 nm, which corresponds to what the human eye perceives as yellow to orange light. The wavelength of the CMB, however, increased as the universe expanded. The CMB is now "seen" at a wavelength of about 2 mm (Hu and White (2004)).

How is the CMB observed now that its wavelength is in the range of the human eye? Observing the CMB has been the subject of several important projects. The Cosmic Background Explorer (COBE), the Wilkinson Microwave Anisotropy Probe (WMAP), Planck, and, most recently, the South Pole Telescope (SPT) are a few examples (Carlstrom, Crawford, and Knox (2015)). Because it is so uniform, the CMB has a very high degree of isotropy and thus causes problems when attempting to measure its anistropic characteristics (Hu and Dodelson (2002)). The detectors would need to be extremely sensitive and well calibrated. SPT-3G+, the next SPT survey (Dibert et al. (2022)), will have the best detectors of any SPT survey to date.

Exploring and preparing an optimal environment for the testing of these future detectors is the ultimate goal of this article.

2 The South Pole Telescope-Sunyaev-Zel'dovich

Because of its extremely dry and stable atmosphere, the South Pole is an ideal region for CMB detection. Normally, the majority of the CMB is absorbed by water in the atmosphere; this is not an issue at the South Pole. The South Pole is likewise around 3,200 meters above sea level. Additionally, at the South Pole, the sun is below the horizon for six months of the year. All of these qualities work together to provide the best view of the cosmos all year (Carlstrom et al. (2011)).

The SPT first started running in 2007 and has gone through three different surveys; with the fourth (SPT-3G+) being planned for 2024 . The South Pole Telescope-Sunyaev-Zel'dovich (SPT-SZ) is the first survey of the SPT that was put to use. It was used from 2007 to 2011 and it detected frequencies of 95, 150, and 220 GHz (Carlstrom et al. (2011)). The University of Chicago currently has the SPT-SZ cryostat and is using it to test the detectors that will be used in the SPT-3G+; an effort led by Karia Dibert, a graduate student at the University of Chicago. A cryostat is essentially a device used to maintain very low temperatures and house the detectors under vacuum. Images of the SPT-SZ cryostat are shown in Figure 5.

The SPT began in 2007 and has gone through three different surveys, with the fourth (SPT-3G+) scheduled for 2024. The South Pole Telescope-Sunyaev-Zel'dovich (SPT-SZ) survey was the first cryostat – a device that maintains extremely low temperatures while housing detectors under vacuum – to use the SPT. Between 2007 and 2011, it observed frequencies of 95, 150, and 220 GHz (Carlstrom et al. (2011)). The University of Chicago now houses the SPT-SZ cryostat and is using it to test the detectors that will be used in the SPT-3G+ survey, an endeavor led by graduate student Karia Dibert. Figure 5 depicts images of the SPT-SZ cryostat.

As previously noted, any anisotropies in the CMB are extremely difficult to detect, therefore the detectors must be extremely sensitive (Hu and Dodelson (2002)). In fact, the detectors are so sensitive that vibrating air molecules could lead to inaccuracies (Sobrin et al. (2022)). To avoid any noise in the data, the cryostat must be vacuumed and the temperature must be extremely low – around 300 mK.

The following section will go over how this was accomplished.

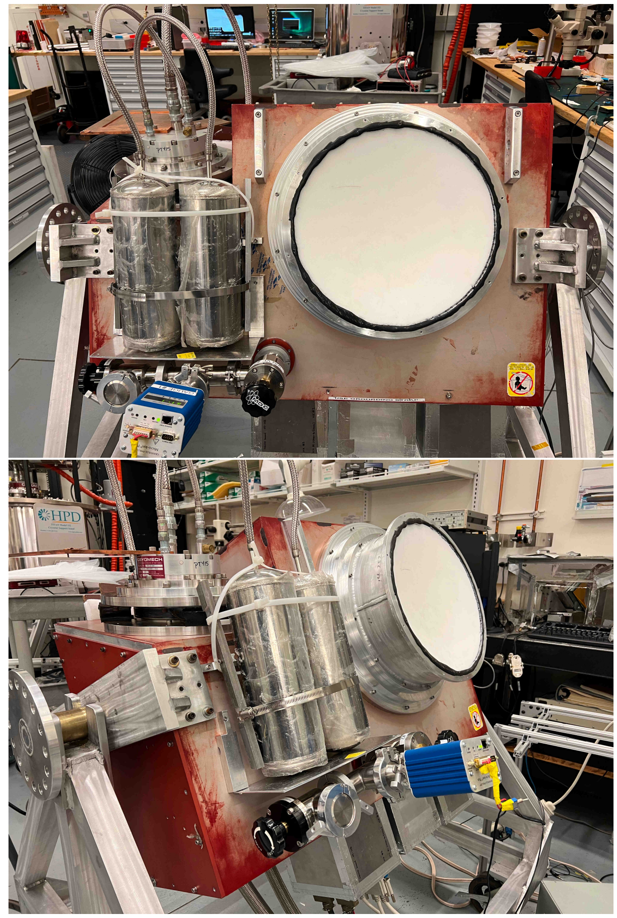

Figure 5: Images show the outside of the SPT-SZ cryostat in the basement of the University of Chicago's William Eckhardt Research Center. Take note of the similarities between the cryostat and a standard camera. They both serve the same purpose, except that the cryostat's detectors are designed to detect microwave light rather than visible light.

3 Cool-down Methodology

A vacuum must be produced in the cryostat before any cooling can take place. This is done to prevent the molecules inside the cryostat from freezing to any of its internal components. An external vacuum is connected to the cryostat via a flex pipe connection to a valve. During the cool-downs, an Agilent Turbo Pumping System-Mobile (TPS-Mobile) (Figure 6) was used. The first step, of course, is to ensure that the cryostat is completely sealed. This involves tightening any loose screws along the outside of the cryostat and ensuring that the cryostat's o-rings are free of fractures and have proper vacuum lubricant. Once the cryostat has been fully sealed and linked to the TPS-Mobile, the valve connecting the cryostat to the TPS-Mobile is fully opened and only the scroll pump is turned on. When the pressure in the cryostat reaches roughly 0.1 Torr, the turbo pump is activated. Following this process prevents any harm to the TPS-Mobile turbo pump. The cryostat is then left on vacuum, and the cooling process begins when the pressure drops to roughly 1e−4 Torr.

To begin cooling the cryostat, a compressor must be attached to the cryostat's pulse tube cryocooler (PTC).

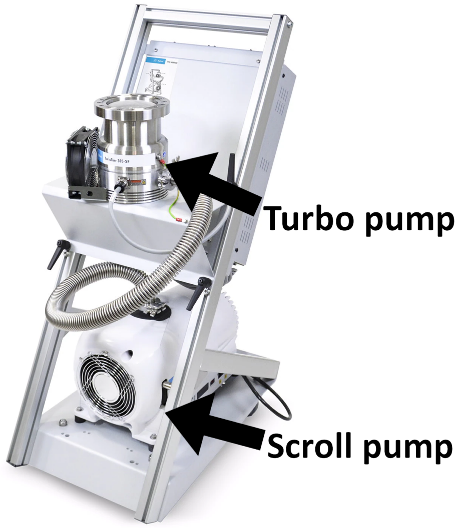

Figure 6: Agilent's Turbo Pumping System-Mobile. The machine's top section is a turbo pump, and its bottom section is a scroll pump. These two vacuums, when combined, can assist the cryostat in reaching pressures as low as 1e−7 Torr.

Figure 7: The PT420 is a Cryomech 2W 4K Pulse Tube Cryocooler. The PT420, like the one used in the SPT-SZ cryostat, has first and second stage capacity. At 55 W, the PT420 can reach 45 K and 4.2 K at 2 W.

The PTC may be seen on the cryostat's left side in the first image in Figure 5. Figure 7 depicts a typical PTC model. PTCs are particularly popular due to their high reliability and low vibration (Wang (2008)). The compressor for this experiment was located in another room and was linked to the cryostat's PTC by a high and low pressure metal pipe. A linear driver motor was also linked to the PTC to control the high and low pressure connections to the compressor. Figure 8 depicts these linkages. The SPT-SZ cryostat is technically a multistage cryostat because the PTC has first and second stage capacities. Figure 9 shows the cryostats' stages. The PTC can get the cryostat to roughly 4 K on its own. It accomplishes this by utilizing the physical features of two helium isotopes: Helium 3 and Helium 4. As stated by Wang, "some 4 K pulse tube cryocoolers have been used for laboratory scale helium liquifiers and reliquifiers to re-liquify the boil off from open liquid helium cryostats," (Wang (2008)). Because the PTC cannot achieve a temperature of 300 mK on its own, an external observer must perform a helium isotope cycle. In the words of Bhatia et al., "by first liquifying Helium 3 then pumping on the Helium 3 bath to reduce the vapour pressure above it, it is possible to lower the temperature of the liquid to [300 mK]" (2013). A python script on a computer attached to the cryoboard (a motherboard that connects the cryostat and a local host) is used to accomplish this. Condensing Helium 3 in a closed vessel and pumping on the resulting Helium 3 gas decreases the total temperature. Superfluidity exists between these two helium isotopes at relatively low temperatures. This occurs when a fluid has no viscosity and hence flows with no loss of kinetic energy. Superfluidity is generally achieved when temperatures get as low as 300 mK.

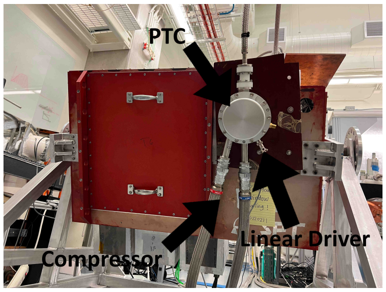

Figure 8: The cryostat's 'back'. All of the connections to the PTC on the cryostat are shown. A short connection connects the linear driver motor to the PTC. A high pressure and a low pressure pipe are connected to the compressor. The linear driver alternates between the low and high pressure connections (when one is opened, the other is closed).

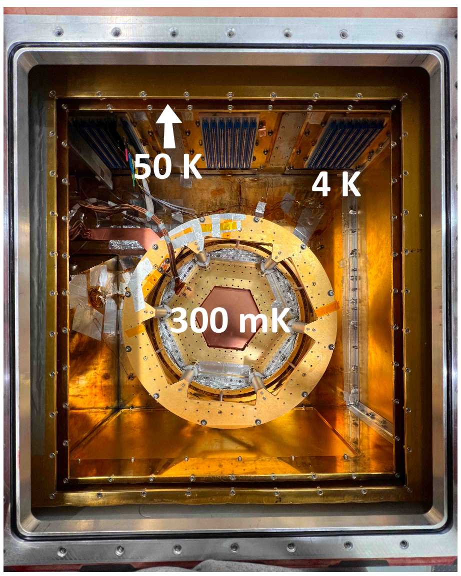

Figure 9: The SPT-SZ features three major stages, which are seen here. The stage in the center is the "ultra-cold stage," which can reach temperatures as low as 300 mK. The region around it is known as the "intra-cold stage," and it has a temperature of roughly 4 K. Both of these levels are in the same 'box,' the middle box. A temperature gradient can occur inside the box because it is exceedingly cold on its own. The 50 K stage is the box around the center box and is the following stage out. It's also the smallest box. The next box outward is the cryostat itself. This box's temperature was not measured during the experiment; it primarily serves as a gradient between ambient temperature and the 50 K stage. Radiation shielding keeps all of the stages apart. Radiation shielding lessens the thermal load on the cooler stages, which would otherwise be unable to keep their temperatures stable.

The best vacuum, cryopumping, is obtained when the cryostat becomes extremely cold. A cryopump, sometimes known as a "cryogenic pump," is a vacuum pump that captures gases and vapours by causing them to condense on a cold surface. When used in conjunction with an external vacuum, a cryopump can reduce pressure to 1e−7 Torr. When this is accomplished, the valve that connects the crysotat to the external vacuum can be closed, and the external can be turned off and unplugged. At this stage, the cryopump achieves self-maintenance.

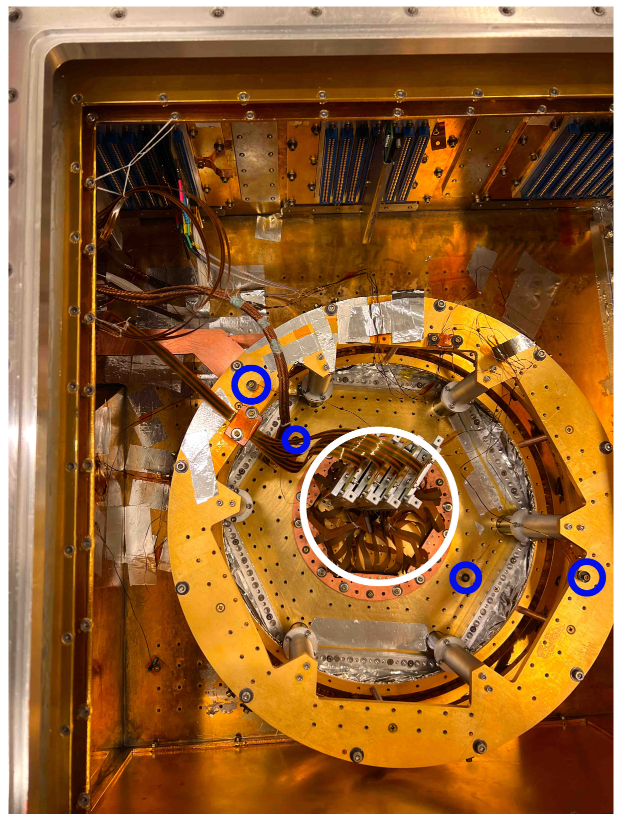

Figure 10: The inside of the cryostat before the third (and last) cool-down. Tyler Natoli, a postdoc at the University of Chicago, built and installed the detector wafer (circled in white). Thermistors are denoted by a blue circle. Thermistors vary their resistance depending on the temperature around them, allowing a computer to read the resistance values and determine the temperature values inside the cryostat.

Temperatures inside the cryostat are measured using thermocouples. They are especially beneficial in these cases since their resistance varies with temperature. Figure 10 depicts thermistors in action. They are connected from the interior to the temperature boards (shown in Figure 11), and from the outside to a computer. A superconducting quantum interface device (SQUID) board connects the detectors to the temperature boards. A SQUID board is an extraordinarily sensitive magnetometer that can detect very small magnetic fields. As a result, they are ideal for detectors that measure very minute oscillations in the CMB, enabling the monitoring of temperature variations, as well as the cryostat's base temperatures.

The following part will go over the temperatures recorded during three different cool-downs. The first cool-down was performed with the cryostat as it was at the start of the summer, the second after introducing an additional zote-foam filter into the cryostat, and the third after inserting a detector wafer into the cryostat. The thermistors remained in the same place throughout each cool-down.

Figure 11: The cryostat's 'bottom'. The temperature boards are white-outlined. To connect these boards to the cryoboard, a gender changer is used. This enables temperature measurements within the cryostat.

4 Temperature Results

While various temperatures were measured during each cool-down (18 in total), the ones that will be highlighted in this part are those at the cryostat's ultra cold stage.

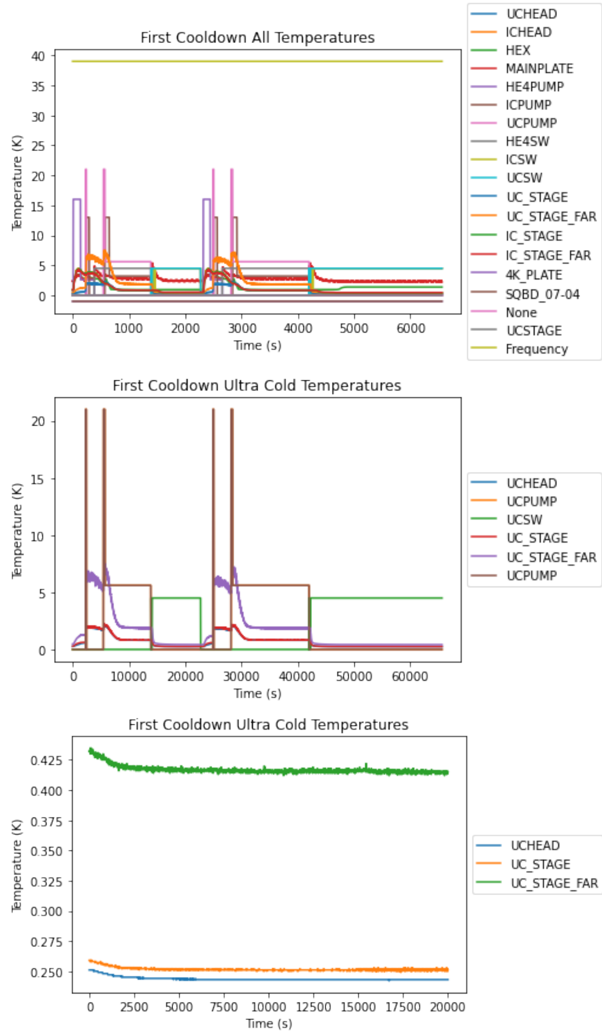

Figure 12: The first cool-down results in terms of temperature. The top plot depicts all of the measured temperatures, the middle plot depicts only the super cold temperatures, and the bottom plot depicts the coldest temperatures over a 2000 second timeframe. This layout will also apply to Figures 13 and 14.

Tyler Natoli created a temperature logger Python script. Every 10 seconds, the logger would take a temperature reading from each thermistor. Unfortunately, it wasn't functioning until midway through the first cool-down. This explains why the greatest temperature in Figure 12 is roughly 40 K rather than 300 K (room temperature). The primary goal of this experiment is to examine the base temperature of each cool-down, which can still be done in this instance. The main takeaway here is that the UCHEAD temperature dropped to 243 mK during the initial cool-down. This first cool-down also doesn't show a lot of noise in the plots; they appear to be rather stable.

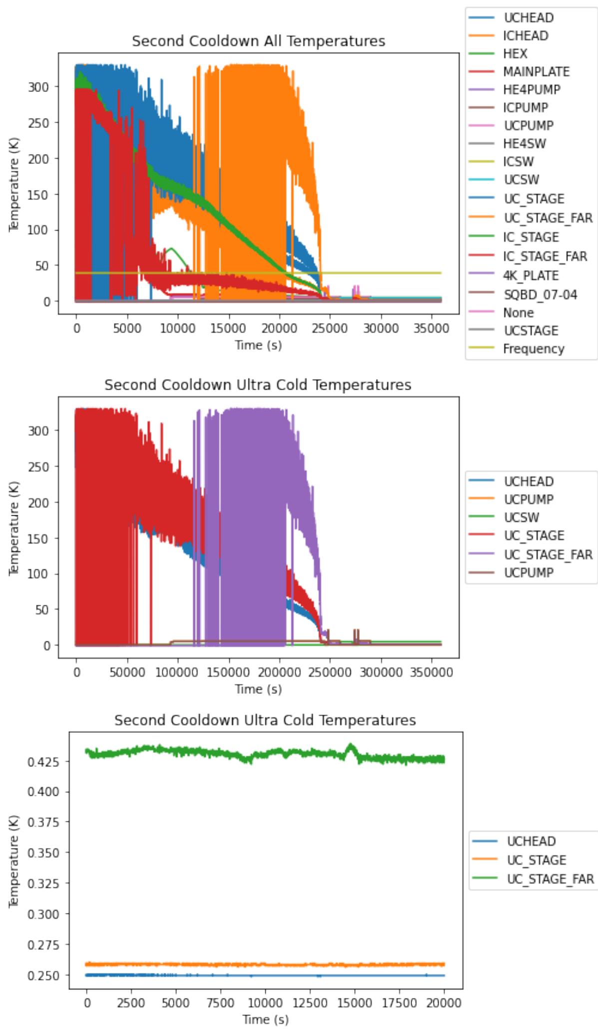

Figure 13: This figure shows the temperature results from the second cool-down. The temperature monitoring began much earlier in the cool-down than it did in the first cool-down, thu temperatures here begin at ambient temperature (about 300 K).

The temperature logger was initiated at the start of the second cool-down, therefore the 300 K temperature displayed on the y-axis of Figure 13 is accurate. The noise inside the cryostat is at its loudest at room temperature, and certain thermistors are not calibrated to measure high temperatures; they are designed to measure low temperatures. When the temperatures drop low enough, as shown in the bottom plot of Figure 13, the data becomes stable. The base temperature during the second cool-down is 249 mK.

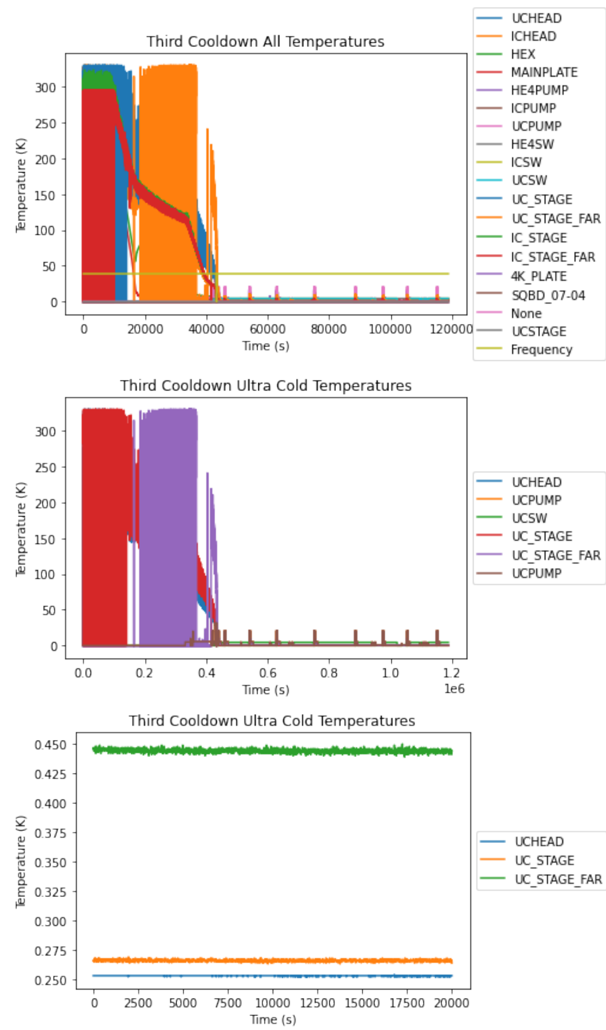

Figure 14: These graphs depict the temperature results from the third cool-down. This is the largest of the three data sets. The goal for this final cool-down was to maintain the cryostat as cold as possible for as long as feasible.

The final cool-down lasted the longest of the three. Because this was the final cool-down and the one with the most devices within the cryostat, the goal was to create a firm base temperature. Figure 14 depicts the same effect as Figure 13 in terms of a very noisy introduction to the data. Again, this is not alarming, but rather expected. The base temperature of the third cool-down is 253 mK, as seen in the bottom plot of Figure 14. Figure 15 compares the base temperatures of all three cooldowns.

Every cool-down, the UCHEAD thermistor is the coldest. As a result, it is the optimum temperature to

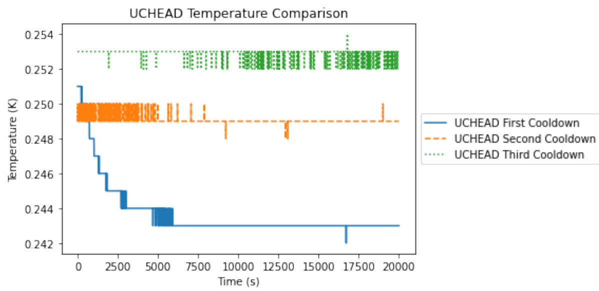

Figure 15: Comparison of base temperatures from all three cool-downs. The graph suggests that adding more devices to the cryostat raises the base temperatures and increases the noise in the data.

compare the three. Figure 15 compares the UCHEAD thermistor after each cool-down. The first cool-down has the lowest base temperature at 243 mK, followed by the second cool-down at 249 mK and the third cool-down at 253 mK. This demonstrates that as more devices are added to the cryostat, the base temperatures rise. Fortunately, all of the base temperatures are far lower than the projected base temperature of 300 mK. It is also worth noting that as the base temperature rises, so does the amount of noise in the data; 243 mK has the least amount of fluctuation and 253 mK has the most. A 1 mK variation, though, is not cause for concern.

5 Conclusions

Although the temperature increased as more devices were added to the cryostat, the final base temperature was significantly lower than projected. The SPT-SZ cryostat has shown to be pressure and temperature stable enough to house and test detector wafers for future SPT surveys. Also, if necessary, the cryostat can hold additional equipment for the instrumentation summer school for graduate students.

6 Acknowledgements

Thank you to Dr. Bradford A. Benson, Dr. Sasha Rahlin, Dr. Tyler Natoli, Dr. Thomas Crawford, and Paul Chichura for all of the guidance this summer. They truly helped me comprehend the project's core framework, and I could not have done it without any of them. Thank you to the South Pole Telescope Collaboration for accepting me as a member of the SPT Group this summer. Finally, I'd like to thank the Materials Research Science and Engineering Center at the University of Chicago for the opportunity to explore the field of astrophysics.

References

Carlstrom, J. E. et al. (2011). “The 10 Meter South Pole Telescope”. In: *Publications of the Astronomical Society of the Pacific* 123 (903), pp. 568–581.

Carlstrom, John E., Thomas M. Crawford, and Lloyd Knox (2015). “Particle physics and the cosmic microwave background”. In: *Physics Today* 68 (3), pp. 28–34.

Dibert, K. et al. (2022). “Development of MKIDs for Measurement of the Cosmic Microwave Background with the South Pole Telescope”. In: *Journal of Low Temperature Physics* 209 (3-4), pp. 363–371.

Hu, Wayne and Scott Dodelson (2002). “Cosmic Microwave Background Anisotropies”. In: *Annual Review of Astronomy and Astrophysics* 40 (1), pp. 171–216.

Hu, Wayne and Martin White (2004). “The Cosmic Symphony”. In: *Scientific American* 290 (2), pp. 44–53.

Sobrin, J. A. et al. (2022). “The Design and Integrated Performance of SPT-3G”. In: *The Astrophysical Journal Supplement Series* 258 (2), p. 42.

Wang, Chao (Mar. 2008). “Intermediate cooling from pulse tube and regenerator in a 4 K pulse tube cryocooler”. In: *Cryogenics* 48, pp. 154–159.